Check for updates

Molecular Omics

Accepted Manuscript

This article can be cited before page numbers have been issued, to do this please use: S. S. Shan, P. F. Wang, J. K. Cheung, F. Yu, H. Zheng, S. Luo, S. P. Yip, C. H. To and C. LAM, *Mol. Omics*, 2022, DOI: 10.1039/D1MO00407G.

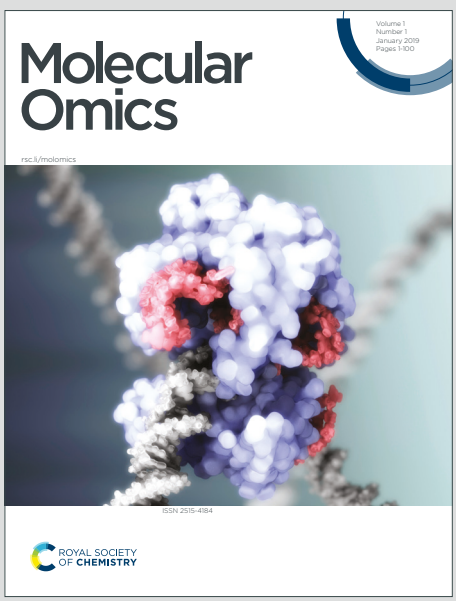

ROYAL SOCIETY OF CHEMISTRY

rsc.li/molomics

The following publication Shan, S. W., Wang, P. F., Cheung, J. K. W., Yu, F., Zheng, H., Luo, S., ... & Lam, T. C. (2022). Transcriptional profiling of the chick retina identifies down-regulation of VIP and UTS2B genes during early lens-induced myopia. Molecular Omics, 18(5), 449-459 is available at https://dx.doi.org/10.1039/D1MO00407G.

View Article Online
DOI: 10.1039/D1MO00407G

Article

Transcriptional profiling of the chick retina identifies down-regulation of *VIP* and *UTS2B* genes during early lens-induced myopia

Sze Wan Shan [1,6,7*], Pan Feng Wang [2,*], Jimmy Ka Wai Cheung [1,6], Fengjuan Yu [3], Hui Zheng [1,4], Shumeng Luo [5], Shea Ping Yip [5,6,7], Chi Ho To [1,6,7§], and Thomas Chuen Lam [1,6,7§]

**Co-first author with equal contribution*

[1] Laboratory of Experimental Optometry, Centre for Myopia Research, School of Optometry, the Hong Kong Polytechnic University, Kowloon, Hong Kong; [2] State Key Laboratory of Ophthalmology, Zhongshan Ophthalmic Center, Sun Yat-Sen University, Guangzhou, China; [3] Increasepharm (HK) Limited; [4] Tianjin Eye Hospital, Tianjin, China; [5] Department of Health Technology and Informatics, The Hong Kong Polytechnic University, Kowloon, Hong Kong; [6] Centre for Eye and Vision Research (CEVR), 17W Hong Kong Science Park, Hong Kong; [7] Research Centre for SHARP Vision (RCSV)

§ Corresponding authors

Dr Thomas, Chuen Lam PhD

HJ537, School of Optometry, The Hong Kong Polytechnic University, Hong Kong

Tel: (852) 27666115 Fax: (852) 27646051 E-mail: thomas.c.lam@polyu.edu.hk

Prof Chi-ho To PhD

HJ 510, School of Optometry, The Hong Kong Polytechnic University, Hong Kong

Tel: (852) 27666102 Fax: (852) 27646051 E-mail: sochto@polyu.edu.hk

View Article Online
DOI: 10.1039/D1MO00407G

Abstract: Gene expression of the chick retina was examined during the early development of lens-induced myopia (LIM) using whole transcriptome sequencing. Monocular treatment of the right eyes with −10 diopter (D) lenses was performed on newly born chicks for one day (LIM-24) or two days (LIM-48), while the contralateral eyes without lenses served as controls. Myopia development was confirmed by demonstrating significant elongation of the optical axis in lens-treated eyes compared with untreated control eyes. RNA was extracted and RNA-seq was performed using Illumina HiSeq™ 2000 platform. Data analysis was carried out on Partek® Flow platform. Using screening criteria of ≥1.30-fold change and a false discovery rate <1%, 11 (five down-regulated and six up-regulated) and 35 differentially expressed genes (six down-regulated and twenty-nine up-regulated) were identified at 24-hour and 48-hour, respectively. Using another cohort for validation, Quantitative PCR confirmed significant changes in the expression of *VIP* and *UTS2B* mRNA ($P < 0.05$) after only 24-hour LIM treatment and numerical changes in the expression for *PCGF5* and *FOXG1*, which were consistent with transcriptome sequencing but did not reach statistical significance. These data suggest that concerted changes of retinal gene expression may be instrumental for initiation of axial elongation and myopia development.

View Article Online
DOI: 10.1039/D1MO00407G

1. Introduction

Myopia has become a significant global public health concern. According to recent reviews, it affected nearly 30% of the world population with the number expected to rise to 50% by 2050 [1]. Myopia is associated with a higher risk of ocular complications leading to vision impairment, causing a significant burden for individuals and society [2]. Understanding the early signals in myopia development will help develop safe, effective, and more targeted therapeutic strategies to stop myopic progression. Myopia is thought to be mainly attributable to excessive growth of the eyeball [3, 4]. Experimental myopia and axial eye growth can be induced by imposing optical defocus or form-deprivation in multiple animal models that share similarities to human myopia development [5]. Among all animal models, the chick is the most widely used and mature experimental model for myopia research today. Early studies have shown that chick myopia can be induced in eyes with dissected optic nerves [6-8] or after injection of tetrodotoxin (TTX) to block neuronal signal transduction to the brain [9], suggesting that the signals relaying altered eye growth originate in the retina. Efforts have been made to investigate the retinal signaling pathways leading to myopia development, but only limited changes at the gene and protein levels have been identified at the onset of myopia [10-12]. A comprehensive picture and fundamental knowledge of gene expression at an early stage of myopia are important in unraveling the pathogenesis of myopia, which could lead to innovative modes of treatment and prevention.

The transcriptome comprises all transcripts, including mRNAs and non-coding RNAs, in one cell or a population of cells under specific conditions. Advances in RNA sequencing (RNA-Seq) technologies, from library preparation through data analysis, have enabled rapid and deep profiling of the transcriptome by direct sequencing of complementary DNAs generated from RNA. Compared with microarray technology, RNA-seq has higher resolution allowing for better quantitative and qualitative detection of gene expression [13, 14]. In addition to data on overall transcript abundance, RNA-seq also provides quantitative information on alternative splicing, novel transcripts, gene structure refinement, and single nucleotide polymorphism (SNP). Transcriptome analysis using RNA-seq has been applied in multiple research fields in basic research, medical research, and drug development. Recently, transcriptome analysis was used to characterize the molecular mechanisms of the

View Article Online
DOI: 10.1039/D1MO00407G

developing mouse lens [15], human lens [16 17]and human photoreceptors in retinal cultures [18], human retinal tissues [19-22], and molecular changes in mouse axonal injury model [23]. RNA-Seq revealed that the human retinal transcriptome is more complex than previously reported. The complexity of retinal transcriptome was not appreciated with cDNA microarrays and Serial Analysis of Gene Expression (SAGE) [24, 25]. RNA-seq was also performed on chicken model recently. For example, in developing chicken retina [26], chicken eyelids [27], and myopic eyes [28-30]. However, to our knowledge, this approach has not yet been applied to the chick model of lens-induced myopia (LIM) at early treatment time points (1 and 2 days after lens wearing) when the defocus signals are first initiated at the retina before other associated structural changes can be measured.

In this study, using the well-established LIM chick model we used in previous studies [31-34], we performed a genome-wide screen of transcriptome regulation comparing myopic and control retina at two early treatment time points in this study, followed by validation of early regulated genes. Gene targets and myopia-associated pathways related to myopia allow the discovery of novel biomarkers involved in myopia development. For example, Apolipoprotein A1 was one of the novel protein biomarkers related to ocular changes found in our previous study [35]. Complementary to our previous proteomics work, the present data focused at early responses when the molecular signals in transcripts first initiated at the retina. This information can provide new therapeutic targets and insights to study possible interventions for the control and treatment of myopia.

Experimental

1.1. Animals

White Leghorn chicks (*Gallus gallus domesticus*) were used and raised at 25°C under a 12/12-hour light/dark diurnal cycle. Food and water were provided *ad libitum*. According to our pre-set two experimental time points, biometric measurements of A-scan was used to determine the success of our LIM model. Only minor discomfort will be experienced during lens wearing and cleansing which lasts for a few seconds each time. Upon daily checking, all chicks were found with myopic changes in the treated eyes. The rearing and

View Article Online
DOI: 10.1039/D1MO00407G

experimental procedures in relation to the use of animals were approved by the Animal Ethics Committee of The Hong Kong Polytechnic University and were in compliance with the ARVO Statement for the Use of Animals in Ophthalmic and Vision Research. As the experimental procedures were well established and the treatment time was short, no animal was found injured or dead before the end of the treatments. The animals were anesthetized using intramuscular injection of 50mg/kg ketamine with 3.5mg/kg xylazine and followed by cardiac perfusion to avoid retinal and chorodial blood contamination under anesthesia. For cardiac perfusion step, the chick was secured on a foam platform and a transverse incision of musculature to the lower rim of rib cage was performed to expose the heart. Forceps were used to grasp the heart near its apex and a 23 gauge needle was inserted, which was connected to a syringe pump, to the left ventricle. The perfusion started using phosphate buffered saline (140 mM NaCl, 10 mM phosphate buffer, and 2.68 mM KCl, pH 7.4 at 25°C) until the clear fluid was observed (about 10ml/min for 5 minutes). Finally, vital tissue harvest of the heart was adopted as a confirmation of euthanasia.

1.2. Lens-induced myopia treatment

To induce lens-induced myopia (LIM), chicks were reared with -10 diopter (D) lenses placed over on the right eyes (RE) on the fourth day after hatching. Two groups of LIM chicks were created: a 24-hour group (n = 8) and a 48-hour group (n = 11), respectively. In both groups, the left eyes (LE) were untreated and served as control eyes. Ocular axial lengths were determined by a high-frequency (30 MHz) A-scan ultrasonography system (Panametrics, Inc., Waltham, MA) before lens-mounting and before dissection. After either one or two days of treatment, transcardial perfusion was performed, and both eyes were enucleated immediately [36] and the retina was isolated and collected. All the procedures were performed by an experienced researcher with ophthalmology training. Samples of all eyes with similar size were collected and stored at liquid nitrogen immediately for subsequent experiments.

1.3. RNA extraction

Total RNA was extracted from each tissue sample with RNeasy Plus Micro kit (Qiagen, Germantown, MD) following the manufacturer's protocol. The purity of RNA was confirmed by determining the ratios of 260/280 nm (between 1.8 and 2.1) on a Nanodrop

View Article Online
DOI: 10.1039/D1MO00407G

ND 2000 (NanoDrop Technologies). RNA integrity was also determined by one percent agarose gel, in which both bands of ribosomal RNAs (18S and 28S) were clearly visible, and the ratio of band intensities (28S:18S) was ≥1.0 (data not shown). The concentrations of diluted RNA samples were also assessed by using UV spectroscopy (260 nm) to make sure that the same amount of materials from all chicks were used in the study. The RNA samples were sent to Beijing Genomics Institute (BGI) for subsequent sequencing with all samples met RIN ≥ 7.0.

1.4. RNA sequencing

After the total RNA extraction and DNase I treatment, magnetic beads with Oligo (dT) were used to isolate mRNA. Mixed with the fragmentation buffer, the mRNA was fragmented into short fragments. Then, cDNA was synthesized using the mRNA fragments as templates. Short fragments were purified and resolved with EB buffer for end reparation and single nucleotide A (adenine) addition. After that, the short fragments were connected with adapters. After agarose gel electrophoresis, suitable fragments around 500bp were selected for use as templates of PCR amplification. Several rounds of PCR amplification with PCR Primer Cocktail and PCR Master Mix were performed to enrich the cDNA fragments. Then the PCR products were purified with Ampure XP Beads (AGENCOURT). During the QC steps, Agilent 2100 Bioanaylzer (Agilent RNA 6000 Nano Kit), and ABI StepOnePlus Real-Time PCR System are used in quantification and qualification of the sample library. At last, the library was sequenced with 90bp single-end reads using Illumina HiSeq™ 2000 platform (Illumina, La Jolla, CA).

Genome alignment, quality control, and differential gene expression were analyzed using cloud-base Partek® Flow and Partek® Genomic Suite (PGS) (Partek, St. Louis, MO). Trimming of raw reads (both ends) was based on a minimum quality score of 20 and minimum read length of 25. Trimmed reads were aligned to the chicken genome galGAL5 using STAR - 2.4.1d [37]. Normalized counts using the controls among all biological samples were analyzed for differential expression with the ANOVA analysis method. Genes were considered to be differentially expressed if they met the stated criteria (False discovery rate (FDR) <1%, P<0.05 and fold change ≥1.30).

1.5 RT-qPCR

View Article Online
DOI: 10.1039/D1MO00407G

Reverse transcription of mRNA to cDNA was performed using High Capacity cDNA Reverse Transcription Kit (Applied Biosystems, Foster City, CA), followed by qPCR using LightCycler 480 SYBR Green I Master (Roche Applied Science, Indianapolis, Illinois) with primers specific for four target genes: vasoactive intestinal peptide (*VIP*), forkhead box G1 (*FOXG1*), Urotensin-2B (*UTS2B*), and polycomb group ring finger 5 (*PCGF5*). Glyceraldehyde 3-phosphate dehydrogenase (*GAPDH)* was set as the internal reference gene (Table 1).

Primers were designed using Primer3 (v.0.4.0). RT-qPCR was performed in 96-well plates on a LightCycler 480 (Roche Applied Science, Indianapolis, IL). A total reaction volume of 10 µl contained five microliters of 2×Taq PCR Master Mix, one microliter of sterile water, two microliters of cDNA template, and one microliter of 10 µM primers (forward and reverse). The thermal cycling conditions were: 95˚C for five minutes followed by 40 cycles of 95˚C for 30 sec, 61˚C for 30 sec, and 72˚C for one minute. Samples were run in triplicate. A melting curve analysis was also performed to determine primer–dimer formation, and non-specific amplification products. A specific PCR product was determined by a single peak on the melting curve. For all genes with GAPDH, PCR efficiencies (E) were determined by analyzing a standard curve ($E = 10^{-1/slope}$) and were tested in order to ensure similar efficiency (E = 1.8 to 2.1). A negative (i.e., no-template) control sample was included in each plate. Data were analyzed using the LC480 software. Differential expression of the targeted genes was analyzed with the student's T-test.

1.6 Statistical analysis

Using Partek® Flow and Partek® Genomic Suite (PGS) (Partek, St. Louis, MO) software, RNA-seq result from each individual eye was normalized among biological groups (n = 3 at each group for both LIM-24 group and LIM-48 group). One-way ANOVA with FDR correction was used to compare the gene quantification data between LIM and control samples in RNA-seq. Genes with *P*-value of ≤0.05 and fold change ≥1.30 were considered as differentially expressed genes. FDR was adopted for multiple testing correction in all cases. For qPCR confirmation test, two-tailed paired Student's t-test was used to compare the screened gene quantification data from a new cohort of animals (n =

View Article Online
DOI: 10.1039/D1MO00407G

5 at LIM-24 group and n=8 for LIM-48 group). Genes with *P*-values ≤ 0.05 were considered as significantly changed between LIM and control chicks for each time point.

2. Results

2.1. Biometric measurements

For biometric measurements, a total of n = 8 and n = 11 were used in the LIM-24 and LIM-48 groups, respectively. An overall change in ocular axial length was evident in the experimental chick eye in response to optical defocus using a -10 D lens, which was consistent with previous studies [34, 35, 38]. After wearing -10 D lenses for 24 hours, a significant increase of both vitreous chamber depth (VCD) and axial length (AXL) was apparent when compared with untreated contralateral eyes (all P <0.05). With a longer lens-wearing time of 48 hours, the elongation of VCD and AXL in lens-wearing eyes continued and remained statistically significant when compared with untreated eyes (both P <0.05). Figure 1 summarizes the changes in all ocular axial dimensions after wearing the -10 D lens for 24 hours (A) and 48 hours (B).

2.2. RNA-seq analysis and gene expression in LIM chick retina

To examine early changes in transcriptome profile, i.e., at initiation of LIM, RNA-seq was performed after 24 hours and 48 hours of lens wear. The total raw reads per sample of retina RNA ranged from 23.3 to 24.5 million were got for RNA-seq analysis. A multi-step workflow was employed for the RNA-seq data analysis using Partek® flow (Figure 2). This included alignment quality analysis/quality control (QA/QC) steps, quantification, normalization, and differential analysis. The pre-alignment QA/QC steps checked the quality of the sequence reads before alignment, while the post-alignment QA/QC tool evaluated the performance of alignment. After the quality check, a built-in quantification step was used to quantify the aligned reads with reference to Gal5 genome using STAR aligner. These counts were normalized using the Reads Per Kilobase per Million mapped reads (RPKM). After QC steps the reads were mapped to the reference genome (galGAL5) of the International Chicken Genome Consortium (Dec 2015, Accession ID: GCF_000002315.4). The total mapped reads per sample of retina RNA ranged from 22.0

View Article Online
DOI: 10.1039/D1MO00407G

to 23.3 million, which amounted to a total of 4,689 identified genes. In the final step, comparison of the groups was performed by one-way ANOVA, followed by Benjamini-Hochberg FDR corrections for multiple testing. Volcano plots were generated to visualize the gene-level results (Figure 3).

Genes were considered to be differentially expressed when the FDR was < 1%, and there was at least a 1.30-fold change in expression with statistical significance. After screening out gene candidates which did not meet those criteria, 11 genes were differentially expressed at the 24-hour time point (five down-regulated and six up-regulated). *FOXG1* was up-regulated (>2.50-fold), and *UTS2B* was down-regulated (<2.13-fold) with large fold changes. For the other nine differentially expressed genes, the fold change in expression was below 1.70. In the LIM-48 chick group, 35 differentially expressed genes were identified, of which six were down-regulated and 29 up-regulated. *UTS2B* was down-regulated by two-fold, while *ELN* was up-regulated (1.85-fold). The differentially expressed genes are shown in Table 2, and Volcano plots of both LIM-24 and LIM-48 chick groups (untreated *vs*. fellow eyes) are shown as Figure 3A and 3B, respectively.

Transcripts of four genes, *UTS2B*, *FOXG1*, *VIP*, and *PCGF5*, were differentially expressed in both the LIM-24 and LIM-48 groups (Table 2). Of these four genes, three had consistent directional change in the LIM-24 and LIM-48 groups. Both *UTS2B* and *VIP* were down-regulated at both time points, while *FOXG1* was up-regulated at both time points. *PCGF5* was found to be up-regulated at 24 hours of LIM, but down-regulated at 48 hours.

2.3. Quantitative PCR (qPCR) of four genes

For real-time qPCR (RT-qPCR), five and eight chicks were used for the LIM-24 group and LIM-48 group, respectively. To validate the results of RNA-seq analysis with RT-qPCR, four genes found to be differentially expressed at both time points, *VIP*, *FOXG1*, *UTS2B*, and *PCGF5* were selected. The results of RT-qPCR partially confirmed the RNA-seq results. Specifically, significant downregulation was confirmed for *VIP* and *UTS2B* transcript levels after 24 hours of lens wear. However, after 48 hours of lens wear, *UTS2B* transcript levels were numerically down-regulated, but the difference did not reach

View Article Online
DOI: 10.1039/D1MO00407G

statistical significance, and *VIP* transcript levels were not notably different from control eyes (Figure 4A and 4B). *FOXG1* transcript levels were numerically increased only at the 48-hour time point, but the difference was not statistically significant (Figure 4C). *PCGF5* transcript levels were numerically increased at both 24 hours and 48 hours in lens-wearing eyes, but the difference to the control group was not statistically significant (Figure 4D).

3. Discussion

Hyperopic defocus induced by a high-power negative lens, if applied sufficiently long, induces myopia in the chick [33, 39-41]. The chick model was introduced by Wallman, Turkel and Trachtman, which is the most widely used animal model for myopia research today [42]. Major advantages of the chick model include relatively large eyes, rapid eye growth, highly sensitive control of the refractive state, excellent optics, active and wide ranges of accommodation, high visual acuity, easy drug delivery by intravitreal injection, friendly and co-operative nature, and inexpensive [43, 44]. Also, its Gene Ontology (GO) is also very similar to the human retina. Young chick is thus an ideal model for studying the visual function and molecular signals in human myopia. In the LIM chick model (-10 D lenses), development of full myopia usually takes more than seven days [39]. It is generally believed that the induced myopic signals are first generated from the retina when the defocus is observed, and the signals will then move across the choroid to the sclera where tissue remodeling takes place at a later stage. To identify early molecular signals that trigger the axial elongation of the eye under defocus, the key objective of this study only focuses on early signals, but not signals at the late stage. Recent ocular proteomics studies suggested the importance of studying early molecular regulations in short-term LIM [31-33, 45]. Recent RNA-sequencing technologies allow sensitive detection and profiling of more up-stream mRNA expression in the myopic eyes [11]. In this study, early time points (24 hours and 48 hours) were selected for transcriptomic analysis in order to detect early gene-expression signals as recent studies pointed to the early protein signals related to myopia and accelerated eye growth that could be identified as early as 3 days [31, 46]. They suggested further studies of myopia biomarkers should focus on an early stage rather than a later stage. As transcripts should be altered earlier than proteins, we studied earlier time points at both 1 and 2 days that were seldom studied in other myopia studies. Actual eye growth at these

View Article Online
DOI: 10.1039/D1MO00407G

early time points is comparatively minor compared to fully developed LIM. The current study's findings for axial eye growth at these early time points were in line with published data and suggested lens treatment had the intended effects on myopia induction. The continuous elongation of VCD and AXL reached significance at the longer exposure time (48-hour) as the choroidal layer recovered some of its thickness over time, which was also observed in other studies [47-49]. This indicated that the initial response of the choroid to defocus signals wears off after a short period of time [50].

VIP is expressed in eyes, where its gene product functions as a peptidergic neuromodulator [51]. In this study, RNA-seq demonstrated reduced *VIP* gene expression after 24-hour and 48-hour LIM treatment, and RT-qPCR confirmed the results after 24 hours of lens wear. Similar findings were observed by the group of McGlinn, who found down-regulation of retinal *VIP* expression after three days of goggles wearing, but not after six hours [52]. *VIP* was also reported to be down-regulated in a meta-analysis of transcriptomic datasets for optically induced myopia of the chick [11]. In that meta-analysis, reduced expression of *VIP* was found at early (≤24 hours of lens myopia induction) and late (>24 hours of myopia induction) time points. Intravitreal VIP injection was found to reduce myopia progression in two chick models of myopia, form deprived myopia (FDM), and eye occlusion , which is consistent with the findings in this study, and suggests that down-regulation of *VIP* is functionally relevant [53]. However, not all studies found that VIP could reduce FDM [54-58]. VIP-mediated prevention of FDM is believed to depend on a signaling cascade involving activation of adenylyl cyclase and production of cyclic adenosine monophosphate (cAMP) [55, 59]. This hypothesis is supported by our earlier finding that the cAMP analogue 8-Bromo-cAMP (8-Br-cAMP) could inhibit LIM development in chicks [35]. Overall, the identification of VIP as a down-regulated gene in LIM is supported by the literature and validates the RNA-seq approach used in this study.

UTS2B, also known as urotensin II-related peptide (URP), was the second gene down-regulated by 24-hour and 48-hour lens wear in the RNA-Seq experiment. Its down-regulation was confirmed via RT-qPCR analysis. *UTS2B* has been shown to play a key role in the neuroendocrine system, behavioral regulation, heart rate, and blood pressure control [60-62]. However, its exact role in the retina and in LIM is not well characterized. Pre-pro-

View Article Online
DOI: 10.1039/D1MO00407G

urotensin II-related peptide (pp-URP II) has been found to be down-regulated in FDM chicks [52]. Pp-URP II, which is a urotensin II paralog precursor was found down-regulated in eyes with both positive- and negative-lenses wear [63]. Overall, there is only limited support in the literature for UTS2B down-regulation in LIM, and the role of UTS2B in LIM is not well characterized. Therefore, further research into the role of UTS2B in the eye and myopia development is warranted.

In this study, *FOXG1* was found up-regulated after both 24 hours and 48 hours of LIM treatment using RNA-seq. This was confirmed by RT-qPCR for the 48-hour time point. *FOXG1* encodes a transcriptional suppressor protein [64, 65], and is expressed mainly in the hypothalamus, optic chiasm, telencephalon, and retina [66-70]. It has been implicated in the development of eye and CNS, and in pattern expression in the CNS, including in the retina [66, 67, 71]. It was also found to play a role in retinal axon growth [72]. FOXG1 mutations result in impaired visual cortical function [73]. However, the role of FOXG1 in myopia is unknown and further research is needed to determine this. Based on its role as a transcriptional suppressor, *FOXG1* has the potential for mediating lens-induced transcriptional changes early after initiation of lens wear. The identification of FOXG1 in this study showed that RNA-seq had the potential to uncover novel differentially regulated genes in the chick LIM model.

RNA-Seq analysis also revealed that transcript levels of *PCGF5* were up-regulated after 24 hours and down-regulated after 48 hours of lens wear. In the RT-qPCR analysis, *PCGF5* was numerically up-regulated after both 24 hours and 48 hours of lens wear, suggesting that *PCGF5* was up-regulated after 24 hours of lens wear, but leaving uncertainty about its regulation at the 48-hour time point. PCGF5 is an epigenetic transcriptional regulator acting with histone-modifier functions, including in embryonic stem (ES) cells, and ES cell differentiation [74]. Polycomb group proteins in general play critical roles in epigenetic regulation of transcription and in orchestrating developmental processes [75, 76]. Therefore, identification of PCGF5 as a differentially regulated transcript in LIM is of interest, suggesting that the RNA-seq method is able to identify differentially regulated genes early, including genes that have the potential to act as master regulators of a myopia-induction transcriptional program. In the chick retina, -10D lens wear may

View Article Online
DOI: 10.1039/D1MO00407G

regulate PCGF5 expression and thereby affect epigenetic modification of histones with subsequent regulation of cell proliferation in the retina. Thus, PCGF5 may be essential for cell proliferation, cell survival, and function of certain retinal cell types. However, the relationship between PCGF5 and myopia is still unclear.

The final differentially expressed transcript of note was *early growth response protein 1* (*EGR1*), which was found to be down-regulated 1.67 fold in LIM eyes only after 48 hours of lens wear, suggesting that it was not differentially expressed at earlier time points. Notably, *Erg1*-knockout mice have a longer axial length and a relative myopic refraction shift when compared with wildtype mice [77]. These findings strongly suggest that down-regulation of *Erg1* is functionally relevant in the chick LIM model. *Erg1* may exert its effects by regulating the expression of transforming growth factor beta (TFG-β), which plays an important role in ocular axial growth [78, 79].

Although the sequencing data showed that *VIP*, *UTS2B*, *PCGF5*, and *FOXG1* were differentially expressed at both time-points, the results of qPCR verification were not fully consistent with the sequencing data. Both techniques offer highly sensitive and reliable gene variant detection. RNA-seq provides higher discovery power to detect novel genes and higher sensitivity to quantify rare variants and transcripts while qPCR can detect known sequences of targeted genes only. RNA-seq is a kind of high-throughput screening test of open-targeted gene expressions for discovery while qPCR can be used for more targeted quantification. To minimize the over-claim that all the significant changes of 4 targets found by RNA-seq are related to myopia, we further use another batch of animals to validate the 4 targted genes. Since we cannot completely rule out the positive findings from the RNAseq data, we only claimed the down-regulation of *VIP* and *UTS2B* genes that were further validated by qPCR as the key findings in our study. Moreover, the correlation between transcript levels and protein abundance could be low. In order to better clarify the mechanism during the onset and development of myopia, it is necessary to investigate and compare the expressions of proteins and RNAs. More work on proteomics expression in myopic chick model is needed to use multi-omics in the retina so both the gene transcripts and proteins in the same tissue can be compared for a more comprehensive understanding of myopia regulation.

View Article Online
DOI: 10.1039/D1MO00407G

4. Conclusion

This study demonstrated that RNA-seq was a useful and informative technique for identifying differentially expressed genes in the retina during early myopia development in chicks. RNA-seq identified genes known to be down-regulated in myopia development, validating the method in myopia research. In addition, RNA-seq identified transcriptional regulator genes that were previously not known to be altered in LIM, suggesting that RNA-seq is a powerful method for unraveling the transcriptional program underlying myopia development as early as 24 hours after LIM in the chick model.

Data Availability: The RNA-seq raw data in this study are available at the Sequence Read Archive (SRA) with accession number PRJNA766764.

Author Contributions: Conceptualization, TC Lam, CH To, SW Shan, and PF Wang; Methodology, SW Shan, PF Wang, Jimmy KW Cheung, FJ Yu, and H Zheng; Data upload and analysis, SW Shan, PF Wang, and Jimmy KW Cheung, SM Luo; Supervision, CH To, and TC Lam; Manuscript writing, SW Shan, Jimmy KW Cheung, and TC Lam; Critical review and revision, SP Yip; Funding support, CH To and TC Lam.

Conflicts of Interest: The authors declare that they have no competing interests.

Acknowledgments: We thank the University Research Facility in Life Sciences (ULS), The Hong Kong Polytechnic University, for providing and maintaining the equipment needed for qPCR and Dr Maureen Valerie Boost (Hong Kong Polytechnic University, Hong Kong) for her diligent proofreading of the article. This research was funded by Henry G Leong Endowed Professorship Fund, PolyU; General Research Fund Research (15104819); The Government of the Hong Kong Special Administrative Region & Innovation and Technology Fund, and Research Centre for SHARP Vision (RCSV).

View Article Online
DOI: 10.1039/D1MO00407G

References

1. B. A. Holden, T. R. Fricke, D. A. Wilson, M. Jong, K. S. Naidoo, P. Sankaridurg, T. Y. Wong, T. J. Naduvilath and S. Resnikoff, *Ophthalmology*, 2016, **123**, 1036-1042.
2. P. Sankaridurg, N. Tahhan, H. Kandel, T. Naduvilath, H. Zou, K. D. Frick, S. Marmamula, D. S. Friedman, E. Lamoureux, J. Keeffe, J. J. Walline, T. R. Fricke, V. Kovai and S. Resnikoff, *Invest Ophthalmol Vis Sci*, 2021, **62**, 2.
3. I. G. Morgan, *Clin Exp Optom*, 2003, **86**, 276-288.
4. S. Vitale, R. D. Sperduto and F. L. Ferris, 3rd, *Arch Ophthalmol*, 2009, **127**, 1632-1639.
5. D. Troilo, E. L. Smith, 3rd, D. L. Nickla, R. Ashby, A. V. Tkatchenko, L. A. Ostrin, T. J. Gawne, M. T. Pardue, J. A. Summers, C. S. Kee, F. Schroedl, S. Wahl and L. Jones, *Invest Ophthalmol Vis Sci*, 2019, **60**, M31-M88.
6. D. Troilo, M. D. Gottlieb and J. Wallman, *Curr Eye Res*, 1987, **6**, 993-999.
7. C. Wildsoet, *Curr Eye Res*, 2003, **27**, 371-385.
8. C. F. Wildsoet and J. D. Pettigrew, *Invest Ophthalmol Vis Sci*, 1988, **29**, 311-319.
9. N. A. McBrien, H. O. Moghaddam, C. L. Cottriall, E. M. Leech and L. M. Cornell, *Vision Res*, 1995, **35**, 1141-1152.
10. E. T. Grochowski, K. Pietrowska, T. Kowalczyk, Z. Mariak, A. Kretowski, M. Ciborowski and D. A. Dmuchowska, *J Clin Med*, 2020, **9**.
11. N. Riddell and S. G. Crewther, *Scientific reports*, 2017, **7**, 9719.
12. X. B. Cai, S. R. Shen, D. F. Chen, Q. Zhang and Z. B. Jin, *Exp Eye Res*, 2019, **188**, 107778.
13. P. A. t Hoen, Y. Ariyurek, H. H. Thygesen, E. Vreugdenhil, R. H. Vossen, R. X. de Menezes, J. M. Boer, G. J. van Ommen and J. T. den Dunnen, *Nucleic Acids Res*, 2008, **36**, e141.
14. U. Nagalakshmi, K. Waern and M. Snyder, *Curr Protoc Mol Biol*, 2010, **Chapter 4**, Unit 4 11 11-13.
15. S. Y. Khan, S. F. Hackett, M. C. Lee, N. Pourmand, C. C. Talbot, Jr. and S. A. Riazuddin, *Invest Ophthalmol Vis Sci*, 2015, **56**, 4919-4926.
16. Z. Wang, D. Su, S. Liu, G. Zheng, G. Zhang, T. Cui, X. Ma, Z. Sun and S. Hu, *BMC Ophthalmol*, 2021, **21**, 152.
17. R. Shparberg, C. U. Dewi, V. Gnanasambandapillai, L. Liyanage and M. D. O'Connor, *Data Brief*, 2021, **34**, 106657.
18. R. Kaewkhaw, K. D. Kaya, M. Brooks, K. Homma, J. Zou, V. Chaitankar, M. Rao and A. Swaroop, *Stem Cells*, 2015, **33**, 3504-3518.
19. Y. Hu, X. Wang, B. Hu, Y. Mao, Y. Chen, L. Yan, J. Yong, J. Dong, Y. Wei, W. Wang, L. Wen, J. Qiao and F. Tang, *PLoS Biol*, 2019, **17**, e3000365.
20. Q. Liang, R. Dharmat, L. Owen, A. Shakoor, Y. Li, S. Kim, A. Vitale, I. Kim, D. Morgan, S. Liang, N. Wu, K. Chen, M. M. DeAngelis and R. Chen, *Nat Commun*, 2019, **10**, 5743.
21. S. T. Schumacker, K. R. Coppage and R. A. Enke, *Sci Data*, 2020, **7**, 199.
22. W. Yan, Y. R. Peng, T. van Zyl, A. Regev, K. Shekhar, D. Juric and J. R. Sanes, *Scientific reports*, 2020, **10**, 9802.
23. M. Yasuda, Y. Tanaka, K. M. Nishiguchi, M. Ryu, S. Tsuda, K. Maruyama and T. Nakazawa, *BMC Genomics*, 2014, **15**, 982.
24. D. Sharon, S. Blackshaw, C. L. Cepko and T. P. Dryja, *Proc Natl Acad Sci U S A*, 2002, **99**, 315-320.
25. M. H. Farkas, G. R. Grant, J. A. White, M. E. Sousa, M. B. Consugar and E. A. Pierce, *BMC Genomics*, 2013, **14**, 486.
26. C. J. Langouet-Astrie, A. L. Meinsen, E. R. Grunwald, S. D. Turner and R. A. Enke, *Sci Data*, 2016, **3**, 160117.

View Article Online
DOI: 10.1039/D1MO00407G

27. H. Yuan, X. Zhang, Q. Zhang, Y. Wang, S. Wang, Y. Li, Y. Zhang, J. Jing, J. Qiu, Z. Wang and L. Leng, *Br Poult Sci*, 2019, **60**, 15-22.
28. N. Riddell, L. Giummarra, N. E. Hall and S. G. Crewther, *Front Neurosci*, 2016, **10**, 390.
29. C. Karouta, R. Kucharski, K. Hardy, K. Thomson, R. Maleszka, I. Morgan and R. Ashby, *Faseb J*, 2021, **35**.
30. L. G. Vocale, S. Crewther, N. Riddell, N. E. Hall, M. Murphy and D. Crewther, *Scientific reports*, 2021, **11**, 5280.
31. F. J. Yu, T. C. Lam, A. Y. Sze, K. K. Li, R. K. Chun, S. W. Shan and C. H. To, *J Proteomics*, 2020, DOI: 10.1016/j.jprot.2020.103684, 103684.
32. J. K. Cheung, K. K. Li, L. Zhou, C. H. To and T. C. Lam, *Data Brief*, 2020, **30**, 105576.
33. F. J. Yu, T. C. Lam, L. Q. Liu, R. K. Chun, J. K. Cheung, K. K. Li and C. H. To, *Scientific reports*, 2017, **7**, 12649.
34. T. C. Lam, K. K. Li, S. C. Lo, J. A. Guggenheim and C. H. To, *Journal of proteome research*, 2007, **6**, 4135-4149.
35. R. K. Chun, S. W. Shan, T. C. Lam, C. L. Wong, K. K. Li, C. W. Do and C. H. To, *Invest Ophthalmol Vis Sci*, 2015, **56**, 8151-8157.
36. J. H. Tao-Cheng, P. E. Gallant, M. W. Brightman, A. Dosemeci and T. S. Reese, *The Journal of comparative neurology*, 2007, **501**, 731-740.
37. A. Dobin, C. A. Davis, F. Schlesinger, J. Drenkow, C. Zaleski, S. Jha, P. Batut, M. Chaisson and T. R. Gingeras, *Bioinformatics*, 2013, **29**, 15-21.
38. J. C. Wang, R. K. Chun, Y. Y. Zhou, B. Zuo, K. K. Li, Q. Liu and C. H. To, *Ophthalmic Physiol Opt*, 2015, **35**, 652-662.
39. E. L. Irving, J. G. Sivak and M. G. Callender, *Ophthalmic Physiol Opt*, 1992, **12**, 448-456.
40. Y. Y. Zhou, R. K. M. Chun, J. C. Wang, B. Zuo, K. K. Li, T. C. Lam, Q. Liu and C. H. To, *Mol Med Rep*, 2018, **18**, 59-66.
41. C. Lam, Doctoral thesis Doctoral thesis, The Hong Kong Polytechnic Universiy. HKSAR, The Hong Kong Polytechnic University, 2007.
42. J. Wallman, J. Turkel and J. Trachtman, *Science*, 1978, **201**, 1249-1251.
43. F. Schaeffel and M. Feldkaemper, *Clin Exp Optom*, 2015, **98**, 507-517.
44. J. Wallman and J. Winawer, *Neuron*, 2004, **43**, 447-468.
45. J. Bian, Y. H. Sze, D. Y. Tse, C. H. To, S. A. McFadden, C. S. Lam, K. K. Li and T. C. Lam, *Int J Mol Sci*, 2021, **22**.
46. S. W. Shan, D. Y. Tse, B. Zuo, C. H. To, Q. Liu, S. A. McFadden, R. K. Chun, J. Bian, K. K. Li and T. C. Lam, *J Proteomics*, 2018, **181**, 1-15.
47. M. E. Fitzgerald, C. F. Wildsoet and A. Reiner, *Exp Eye Res*, 2002, **74**, 561-570.
48. D. Wang, R. K. Chun, M. Liu, R. P. Lee, Y. Sun, T. Zhang, C. Lam, Q. Liu and C. H. To, *PLoS One*, 2016, **11**, e0161535.
49. J. Wallman, C. Wildsoet, A. Xu, M. D. Gottlieb, D. L. Nickla, L. Marran, W. Krebs and A. M. Christensen, *Vision Res*, 1995, **35**, 37-50.
50. D. S. Hammond, J. Wallman and C. F. Wildsoet, *Ophthalmic Physiol Opt*, 2013, **33**, 215-226.
51. J. Troger, G. Kieselbach, B. Teuchner, M. Kralinger, Q. A. Nguyen, G. Haas, J. Yayan, W. Gottinger and E. Schmid, *Brain Res Rev*, 2007, **53**, 39-62.
52. A. M. McGlinn, D. A. Baldwin, J. W. Tobias, M. T. Budak, T. S. Khurana and R. A. Stone, *Invest Ophthalmol Vis Sci*, 2007, **48**, 3430-3436.
53. A. I. Cakmak, H. Basmak, H. Gursoy, M. Ozkurt, N. Yildirim, N. Erkasap, M. D. Bilgec, N. Tuncel and E. Colak, *Int J Ophthalmol*, 2017, **10**, 211-216.
54. U. Mathis and F. Schaeffel, *Graefes Arch Clin Exp Ophthalmol*, 2007, **245**, 267-275.

View Article Online
DOI: 10.1039/D1MO00407G

55. M. H. Makman, J. H. Brown and R. K. Mishra, *Adv Cyclic Nucleotide Res*, 1975, **5**, 661-679.
56. J. Rymer and C. F. Wildsoet, *Vis Neurosci*, 2005, **22**, 251-261.
57. R. L. Seltner and W. K. Stell, *Vision Res*, 1995, **35**, 1265-1270.
58. L. He, M. R. Frost, J. T. Siegwart, Jr. and T. T. Norton, *Exp Eye Res*, 2018, **168**, 77-88.
59. Z. Wang, M. Gerstein and M. Snyder, *Nat Rev Genet*, 2009, **10**, 57-63.
60. S. A. Douglas, D. Dhanak and D. G. Johns, *Trends Pharmacol Sci*, 2004, **25**, 76-85.
61. H. Vaudry, J. C. Do Rego, J. C. Le Mevel, D. Chatenet, H. Tostivint, A. Fournier, M. C. Tonon, G. Pelletier, J. M. Conlon and J. Leprince, *Ann N Y Acad Sci*, 2010, **1200**, 53-66.
62. H. Vaudry, J. Leprince, D. Chatenet, A. Fournier, D. G. Lambert, J. C. Le Mevel, E. H. Ohlstein, A. Schwertani, H. Tostivint and D. Vaudry, *Pharmacol Rev*, 2015, **67**, 214-258.
63. R. Schippert, F. Schaeffel and M. P. Feldkaemper, *Mol Vis*, 2008, **14**, 1589-1599.
64. J. Yao, E. Lai and S. Stifani, *Mol Cell Biol*, 2001, **21**, 1962-1972.
65. N. Marcal, H. Patel, Z. Dong, S. Belanger-Jasmin, B. Hoffman, C. D. Helgason, J. Dang and S. Stifani, *Mol Cell Biol*, 2005, **25**, 10916-10929.
66. S. Huh, V. Hatini, R. C. Marcus, S. C. Li and E. Lai, *Dev Biol*, 1999, **211**, 53-63.
67. C. L. Dou, S. Li and E. Lai, *Cereb Cortex*, 1999, **9**, 543-550.
68. V. Fotaki, T. Yu, P. A. Zaki, J. O. Mason and D. J. Price, *J Neurosci*, 2006, **26**, 9282-9292.
69. V. Hatini, W. Tao and E. Lai, *J Neurobiol*, 1994, **25**, 1293-1309.
70. R. C. Marcus, K. Shimamura, D. Sretavan, E. Lai, J. L. Rubenstein and C. A. Mason, *The Journal of comparative neurology*, 1999, **403**, 346-358.
71. S. Xuan, C. A. Baptista, G. Balas, W. Tao, V. C. Soares and E. Lai, *Neuron*, 1995, **14**, 1141-1152.
72. N. M. Tian, T. Pratt and D. J. Price, *Development*, 2008, **135**, 4081-4089.
73. E. M. Boggio, L. Pancrazi, M. Gennaro, C. Lo Rizzo, F. Mari, I. Meloni, F. Ariani, A. Panighini, E. Novelli, M. Biagioni, E. Strettoi, J. Hayek, A. Rufa, T. Pizzorusso, A. Renieri and M. Costa, *Neuroscience*, 2016, **324**, 496-508.
74. W. Zhao, Y. Huang, J. Zhang, M. Liu, H. Ji, C. Wang, N. Cao, C. Li, Y. Xia, Q. Jiang and J. Qin, *The Journal of biological chemistry*, 2017, **292**, 21527-21537.
75. J. M. Gahan, F. Rentzsch and C. E. Schnitzler, *Proc Natl Acad Sci U S A*, 2020, **117**, 22880-22889.
76. M. Yao, X. Zhou, J. Zhou, S. Gong, G. Hu, J. Li, K. Huang, P. Lai, G. Shi, A. P. Hutchins, H. Sun, H. Wang and H. Yao, *Nature Communications*, 2018, **9**, 1463.
77. R. Schippert, E. Burkhardt, M. Feldkaemper and F. Schaeffel, *Invest Ophthalmol Vis Sci*, 2007, **48**, 11-17.
78. B. Rohrer and W. K. Stell, *Exp Eye Res*, 1994, **58**, 553-561.
79. S. Honda, S. Fujii, Y. Sekiya and M. Yamamoto, *Invest Ophthalmol Vis Sci*, 1996, **37**, 2519-2526.

View Article Online
DOI: 10.1039/D1MO00407G

Figure and Table legends

Figure 1. Changes of ocular components (ACD: anterior chamber depth, LT: lens thickness, VCD: vitreous chamber depth, AXL: from the front of cornea to the front of retina) after -10 D lenses wearing for 24 hours (A, n = 8) and 48 hours (B, n = 11). *P <0.05; *** P <0.01, paired T-test.

Figure 2. Adopted workflow in Partek® Flow Tool.

Figure 3. Volcano plots of the genes quantified during Partek analysis comparing (A) one day and (B) 2 days after lens-wearing (untreated *vs*. fellow eyes). Each point represents the difference in expression (fold-change) between the untreated and fellow eyes. Vertical axis indicates p values for observed differences in transcript abundance. NC indicates no difference in transcript abundance, positive numbers indicate relatively higher transcript abundance in lens wearing [36] eyes, and negative numbers indicate higher transcript abundance in untreated (left) eyes. Lines indicate threshold settings for differentially expressed genes. Green dots indicate genes that are down-regulated in LIM; red dots indicate genes that are up-regulated in LIM. The left panel shows results after 24 hours of lens wearing, the right panel shows results after 48 hours of lens wearing.

Figure 4. Relative change in transcript level expression after lens-wearing for 24 hours (n = 5) and 48 hours (n = 8), as measured by RT-qPCR. Four selected genes (A) UTS2B, (B) VIP, (C) FOXG1, and (D) PCGF5 were tested and compared with their corresponding fellow eye normalized to GAPDH. Error bars represent standard error of the mean. **P ≤0.01; student T-test.

Table 1. Primers for target genes

Table 2. Differentially expressed genes identified by RNA-seq analysis of chick retina in LIM-24 and LIM-48 groups. Normalized counts (fold expression) are shown for transcripts

View Article Online
DOI: 10.1039/D1MO00407G

which have statistically significant different expression compared to untreated groups and have a FDR < 1%.

View Article Online
DOI: 10.1039/D1MO00407G

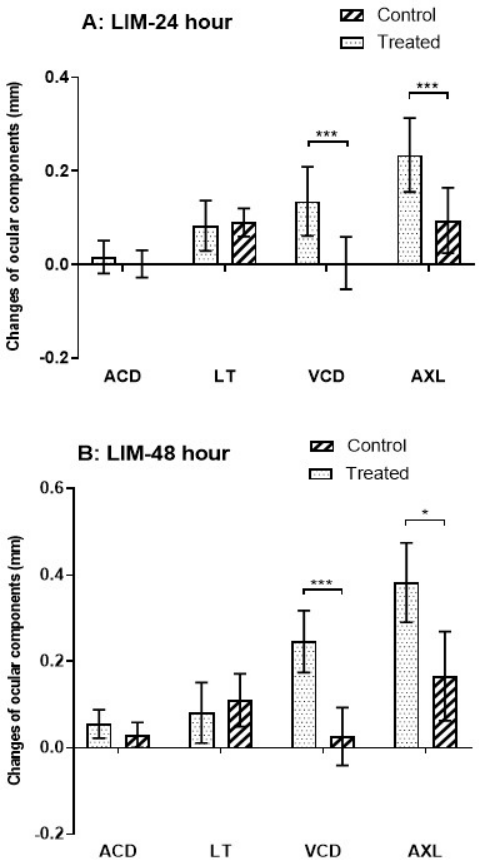

190x254mm (96 x 96 DPI)

View Article Online
DOI: 10.1039/D1MO00407G

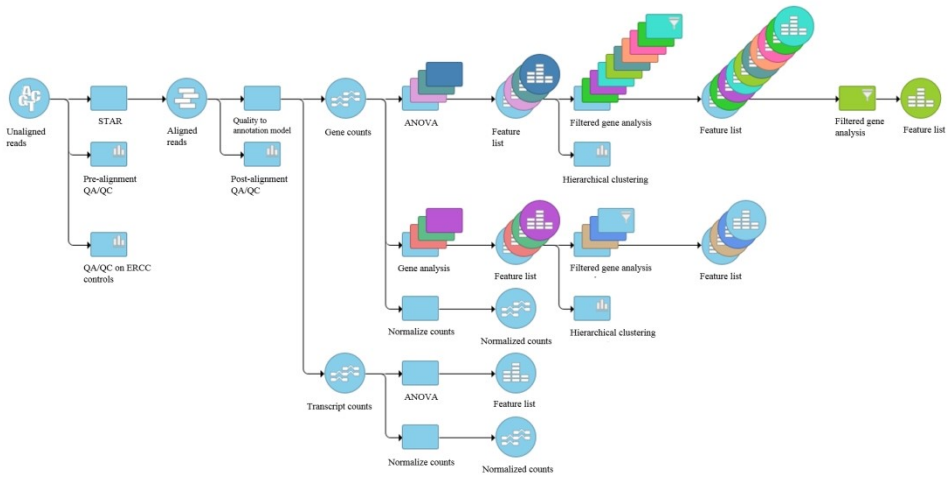

339x181mm (150 x 150 DPI)

View Article Online
DOI: 10.1039/D1MO00407G

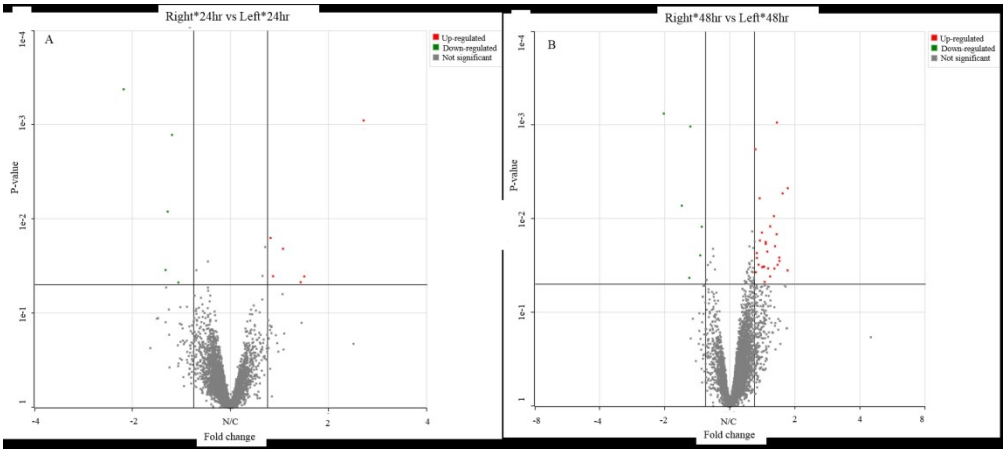

340x151mm (150 x 150 DPI)

View Article Online
DOI: 10.1039/D1MO00407G

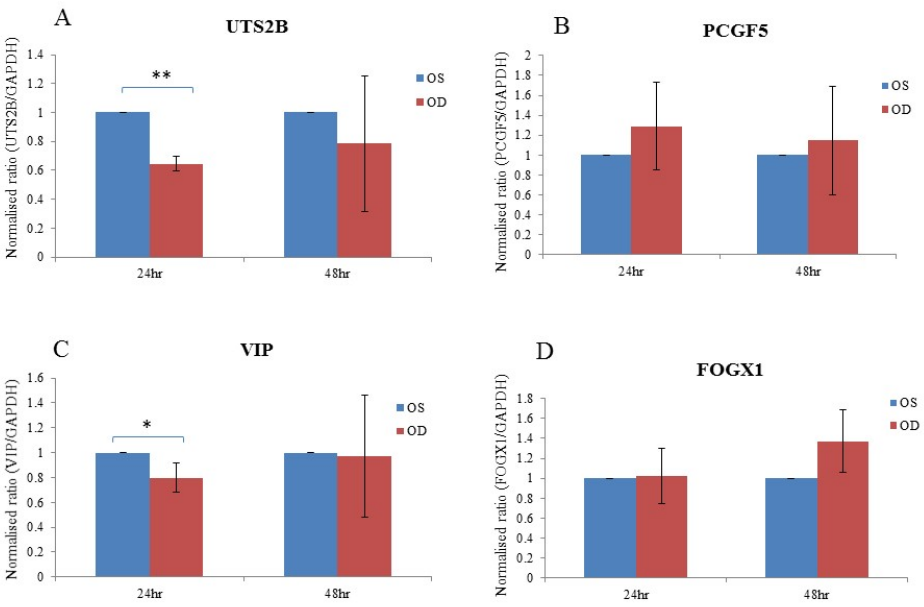

254x190mm (96 x 96 DPI)

View Article Online
DOI: 10.1039/D1MO00407G

Gene	Forward primer (5'>3')	Reverse primer (5'>3')
VIP	ACGAGTTAGCTCCCAGGACA	CCTCGAAGTTTGGCTGGA
FOXG1	AGGAGGGCGAGAAGAAGAAC	ACTCGTAGATGCCGTTGAGC
UTS2B	CTGCACCACAGCCAAGTCTA	GTATGGTGGCAGCAGTCTGA
PCGF5	CAATGACTGTCCCAGGTGTG	GCAGTTCCTGCTCTCGAAGT
*GAPDH**	GGGTGGTGCTAAGCGTGTTA	ACGCTGGGATGATGTTCTGG

* internal reference gene

Gene ID	Gene Name	Fold average LIM-24: LIM eye vs Fellow eye --- LIM-48: LIM eye vs Fellow eye	*P* value LIM-24: LIM eye vs Fellow eye --- LIM-48: LIM eye vs Fellow eye
UTS2B	urotensin 2B	-2.13 --- -2.03	0.0004 --- 0.001
VIP	vasoactive intestinal peptide	-1.51 --- -1.53	0.0013 --- 0.001
FOXG1	forkhead box G1	2.56 --- 1.85	0.0009 --- 0.036
PCGF5	polycomb group ring finger 5	1.33 --- -1.35	0.0159 --- 0.012
DUSP4	dual specificity phosphatase 4	-1.56 --- N/A	0.0083 --- N/A
HTR2A	5-Hydroxytryptamine Receptor 2A	-1.45 --- N/A	0.0471 --- N/A
FST	Follistatin	-1.58 --- N/A	0.0348 --- N/A
RAB23	Ras-related protein Rab-23 precursor	1.35 --- N/A	0.0405 --- N/A
IGF1	Insulin-like growth factor 1	1.45 --- N/A	0.0207 --- N/A
ZIC1	Zic family member 1	1.64 --- N/A	0.0468 --- N/A
BRCA1	BRCA1, DNA Repair Associated	1.68 --- N/A	0.0407 --- N/A
EGR1	Early growth response protein 1	N/A --- -1.67	N/A --- 0.007
PRORSD1P	Prolyl-TRNA Synthetase Associated Domain Containing 1, Pseudogene	N/A --- -1.54	N/A --- 0.043
FOS	Fos Proto-Oncogene, AP-1 Transcription Factor Subunit	N/A --- -1.37	N/A --- 0.025
NEUROD4	Neuronal Differentiation 4	N/A --- 1.31	N/A --- 0.002
TMEM129	Transmembrane Protein 129	N/A --- 1.32	N/A --- 0.037
PC	Pyruvate Carboxylase	N/A --- 1.33	N/A --- 0.023
AMDHD2	Amidohydrolase Domain Containing 2	N/A --- 1.33	N/A --- 0.026
SLC16A2	Solute Carrier Family 16 Member 2	N/A --- 1.36	N/A --- 0.031
SMYD4	SET And MYND Domain Containing 4	N/A --- 1.37	N/A --- 0.006
MRPL34	Mitochondrial Ribosomal Protein L34	N/A ---	N/A ---

		1.37	**0.017**
TAF11	**TATA-Box Binding Protein Associated Factor 11**	**N/A** **----------** **1.40**	**N/A** **----------** **0.014**
ORC6	**Origin Recognition Complex Subunit 6**	**N/A** **----------** **1.41**	**N/A** **----------** **0.033**
RAD9A	**RAD9 Checkpoint Clamp Component A**	**N/A** **----------** **1.43**	**N/A** **----------** **0.032**
ATP6V0D2	**ATPase H+ Transporting V0 Subunit D2**	**N/A** **----------** **1.44**	**N/A** **----------** **0.032**
TOMM6	**Translocase Of Outer Mitochondrial Membrane 6**	**N/A** **----------** **1.45**	**N/A** **----------** **0.047**
EDN2	**Endothelin 2**	**N/A** **----------** **1.46**	**N/A** **----------** **0.018**
TMEM138	**Transmembrane Protein 138**	**N/A** **----------** **1.46**	**N/A** **----------** **0.019**
SLC17A9	**Solute Carrier Family 17 Member 9**	**N/A** **----------** **1.49**	**N/A** **----------** **0.022**
ACYP1	**Acylphosphatase 1**	**N/A** **----------** **1.50**	**N/A** **----------** **0.034**
IMMP2L	**Inner Mitochondrial Membrane Peptidase Subunit 2**	**N/A** **----------** **1.53**	**N/A** **----------** **0.041**
PRR5	**Proline Rich 5**	**N/A** **----------** **1.53**	**N/A** **----------** **0.012**
PHB	**Prohibitin**	**N/A** **----------** **1.60**	**N/A** **----------** **0.009**
LIPT1	**Lipoyltransferase 1**	**N/A** **----------** **1.60**	**N/A** **----------** **0.034**
CCND3	**Cyclin D3**	**N/A** **----------** **1.62**	**N/A** **----------** **0.020**
VAMP1	**Vesicle Associated Membrane Protein 1**	**N/A** **----------** **1.64**	**N/A** **----------** **0.015**
RASL10A	**RAS Like Family 10 Member A**	**N/A** **----------** **1.65**	**N/A** **----------** **0.001**
SNRPN	**Small Nuclear Ribonucleoprotein Polypeptide N**	**N/A** **----------** **1.66**	**N/A** **----------** **0.031**
CDK1	**Cyclin Dependent Kinase 1**	**N/A** **----------** **1.69**	**N/A** **----------** **0.026**
MRPS21	**Mitochondrial Ribosomal Protein S21**	**N/A** **----------** **1.69**	**N/A** **----------** **0.028**
RBP5	**Retinol Binding Protein 5**	**N/A** **----------** **1.75**	**N/A** **----------** **0.005**
ELN	**Elastin**	**N/A** **----------** **1.85**	**N/A** **----------** **0.005**

Table I. Differentially expressed genes identified by RNA-seq analysis of chick retina in LIM-24 and LIM-48 groups. Normalized counts (fold expression) are shown for transcripts which have statistically significant different expression compared to untreated groups and have a FDR < 1%.

View Article Online
DOI: 10.1039/D1MO00407G